

To Dr. Gkioulidou, Topical Editor

I very much appreciate the critical review of our manuscript. Substantial revisions have accordingly been made. The following Comment/Response format addresses each issue. Relevant changes in the manuscript are denoted in bold type with line numbers.

Point-by-point replies to the comments raised by Referee, a list of all relevant changes and marked-up manuscript are given below.

Comment 1:

“The manuscript does an exceptionally poor job of describing what the current understanding is - both observationally and in terms of models. And the specific problem to be addressed is also poorly articulated.”

Response:

Section 1 for the “introduction” was rewritten and section 6 for “summary and discussion” were newly added to clarify the aims and the results of this work.

Comment 2:

“An attempt at clarifying the main problem is added in lines 23-27. This refers to the balloon-measured E-fields, Ba release experiments, and radar studies from the 1970s. As a reader, I am simply not convinced that those studies have led the community to the idea that the poleward motion of auroras travelling at different rates than the equatorward drifts is at all an unanswered question. Surely the author can produce references that have been published over the past 40 years that may have explained these observations?”

Response:

Please refer to the following sentences added in Lines 31-38 of the section 1 (Introduction): “To account for the difference in propagation directions, it was suggested that the primary sources of auroral particles are in the magnetospheric plasmas and they developed in terms of propagation of rarefaction wave in the tail [Chao et al., 1971; Liu et al., 2012], tailward regression/braking of the fast earthward flows referred to as BBFs [Shiokawa et al., 1997; Haerendel, 2015], and onset instability of

inner plasma sheet pressure [Nishimura et al., 2010]. It is suggested that substorm and poleward expansion of auroras were initiated and amplified at the substorm onset by the BBFs arriving at the inner boundary of plasma sheet from the tail [Kepko et al., 2004; Angelopoulos et al., 2008; Machida et al., 2009].”

Comment 3:

“There was an addition of two sentences describing the current understanding on poleward propagation of the substorm auroras. Unfortunately, the explanation is too brief, with no references given and is substantially incorrect. A tailward moving reconnection site is not needed for poleward motion in the reconnection-based model -- simply having reconnection progress to the lobes is enough.”

Response:

Please refer to our above response in Comment 2 for our understanding on poleward propagation of the substorm auroras. Reconnection progress is not included in our explanation, but it may be the subject of another paper, Lines 257-261.

Comment 4:

“There is a very alarming trend in this paper where it seems that every citation of facts relating to observations or causative mechanisms are to the author's own previous publications -- none of which I am familiar with. There certainly are other studies on the aurora and Pi2s, etc. that are relevant to the current topic. It is completely inappropriate not to cite these many other papers.”

Response:

I tried to include as many relevant works as possible. In the previous version of the manuscript, I perhaps too narrowly focused on my own studies to explain the role of low latitude Pi2 pulsations in the substorms. In this revised version, I have remained only more essential references to my work.

Comment 5:

“The new section #2 does not provide any confidence at all in the assertions being made. Use of the T89 Kp 4 model to map results is notoriously untrustworthy. The results may or may not be correct --

which doesn't really tell us anything. There are also many facts definitively stated about Pi2s that by themselves warrant much more observational support than is given here. Inclusion of equation (1) is unnecessary since its context is completely lost on the reader. The conclusions drawn from this equation in lines 71-73 require far more convincing explanation than is given. The remainder of this section (on ballooning) is unclear. Is this a new idea? Existing idea? Is it based on models, theory, observations?

The final sentence of this section is typical of the confusing and unsupported claims in the paper; "The convection surge occurred once in the initial pulse of Pi2 pulsation but is not repeated in the following pulses." This statement seems important, but it is incomprehensible to me. How does the author know this? Is this referring to the Rubtsov study? What was that study? Did they demonstrate that this was a universal finding for substorms? How does this relate to the rest of the current paper? None of this is made clear."

Response:

(1) Please refer to the following sentences in Lines 64-71, "We can postulate the onset scenario that Bursty Bulk Flows (BBFs) reaching the geosynchronous orbit activated preonset auroras in lower latitudes by the transmission of electric fields from the dipolarization front (DF) embedded in the initial pulse of the BBF [Runov et al., 2011]. These transient electric fields were observed by the geosynchronous satellite as the convection enhancement of the plasma sheet electrons due to local breakdown of the last open trajectories of plasma sheet electrons [Thomsen et al., 2002]. The convection enhancement occurred in all-sky image coincident with the onset of bead-like rippling that leads to the breakups at equatorward latitudes [Saka et al., 2014]."

We suppose that the use of T89 model for field line mapping may be acceptable for the present purpose.

(2) Equation (1) and sentences relating to the ballooning instability were eliminated.

(3) Please refer to the following sentences in Lines 71-79, "In the Pi2 pulses following the initial pulse, an auroral surge was observed in all-sky images between 66°N to 74°N in geomagnetic latitudes referred to as Poleward Boundary Aurora Surge (PBAS) [Saka et al., 2012]. They propagated eastward or westward at the poleward boundary of the auroral zone and were interpreted as an auroral manifestation of flow bifurcation of BBFs. In this onset scenario, the field line dipolarization finished in the initial pulse of the Pi2 pulsations, increasing field line inclination in a step-like manner for Goes5, and generating transient pulses for Goes6. The convection surge occurred once in the initial pulse of BBFs (DF) but is not repeated in the following pulses in the BBF train. This correlation suggests that auroral breakup may not repeat in the Pi2 wave packet but occurred at its initial pulse."

Comment 6:

“Section #3 has a paragraph added, but it is also unclear. In line 83 it is stated that "It is reasonable to assume..." Why is it reasonable to assume this? Where does the surge come, from? Why would the high latitude end not expand as stated? Why would the flows be confined as stated? There are simply too many unsupported statements here. And then there is only a single reference to the author's own 2014 publication.”

Response:

Please refer to the following sentences in Lines 64-71 in section 2 for the explanation of the convection surge; its location and onset timing. “The convection surge came from the dipolarization front at the leading edge of BBFs referred to as DF [Runov et al., 2011]. They often appeared at the geosynchronous altitudes as convection enhancement of plasma sheet electrons due to local breakdown of the last open trajectories of plasma sheet electrons [Thomsen et al., 2002]. It appeared in all-sky image coincident with the onset of bead-like rippling that leads to the breakups at equatorward latitudes [Saka et al., 2014].”

Comment 7:

“Section 4 is all bold-faced implying that there are major modifications to the manuscript, but much of it seems identical. I am not sure what has been changed there. Also, equation (6) is from Kelley's text book. Please indicate where in the textbook it can be found. This section also still reads more like facts are being disclosed rather than like an idea is being proposed. I don't know what's known or what's being proposed from this.”

Response:

(1) Steady state flow came from (2.34) in [Kelley, 1989]. Eliminating the second term in the left-hand side of (2.34), we have equation (6) for the parallel flows. It can be applied for both collisional and collisionless cases.

(2) We proposed that compressional ionosphere created the ion outflows and inverted-V type electron accelerations through the excitation of ion acoustic wave in the ionosphere. This idea is new because the ionosphere has been previously considered an inhomogeneous but incompressive medium.

Comment 8:

“Section 5 is also all bold-faced making it difficult to see what has actually been changed.”

Response:

No change was made in this section.

Comment 9:

“The conclusion is still not supported by the body of the paper. I remain unconvinced that "this scenario, analogous to traffic flow of cars on the crowded roads, partly explains the discrepant time history of the auroras which is often described as the auroras expand opposite to that of plasma drift in the ionosphere." The author claims this, but there are many unsupported components that go into the scenario. A rather disturbing aspect of the paper is that it really still does not articulate what the problem is. Citing a few papers from the 1970's is not adequate here -- note that BBFs, streamers, and their relationship, etc were not known to those authors.

Also, the manuscript is completely devoid of any meaningful description of what the auroral observations really show during substorms. In re-reading this paper many times, my guess (and I have to stress here it is just a guess) is that the author is trying to explain the following observational scenario; a) a BBF-associated streamer propagates equatorward, b) as it interacts with the equatorial region, the presumed density accumulations described in the proposed scenario lead to poleward propagation of the auroras, c) this explains the hypothesized substorm sequence described by Nishimura et al.

If this is the intent of the currently proposed scenario, it is not at all clear from what is written. In addition, it is almost certainly incorrect. The types of events showing rapid poleward motion in response to streamers (the so-called contact breakups discovered by Oguti in the 1970s) tend to be explosive in nature, not just like a sand pile building up or tail lights propagating backward. (Note that this is also a major problem with the flow-braking model.) In addition, as I stated above and in my previous review, the scenario proposed here (as well as the Nishimura one) does not adequately describe things like plasmoid releases that are known to occur with substorms.

Once again, I suggest that the author rewrite the manuscript in a manner that the reader can understand what problem it is that is actually trying to be addressed. I feel that there are interesting and possibly important issues raised by the proposed scenario, but the presentation and conclusions are still very misguided. Below is a suggested outline of topics to cover.”

Response:

(1) This report described the auroral expansion in terms of: (1) the BBF triggering the convection surge by electric fields in DF; (2) projections of these electric fields to the ionosphere; (3) creation of the compressibility in the ionosphere by the electric field drifts; (4) excitation of ion acoustic wave by the compression; (5) generation of parallel electric fields by ion acoustic wave; (6) nonlinear evolution of the compressibility for the poleward expansion of auroras. The auroral expansion was described in this acoustic regime which we believe a new scenario not proposed previously.

(2) Characteristic speed of the auroral formation was reported to be 5-8 km/s independent of the spatial scale of the auroras [Oguti, *Metamorphoses of aurora*, *Memoirs of National Institute of Polar Research: series A, aeronomy*, 12, 1-101, 1975]. If we can use this velocity as a speed of poleward expansion, the total electric fields of the order of 300 mV/m may be required in the auroral ionosphere. The electric fields from DF (5 mV/m at $B=30$ nT) create incident electric fields of the order of 200 mV/m by the projections into the auroral ionosphere ($B=50000$ nT). If the Alfvén conductance was larger than the height integrated Pedersen conductance, total electric fields (sum of incident and reflected electric fields) may increase to 300 mV/m. These electric fields produce poleward expansion velocity of the order of 6 km/s. This is consistent with Oguti’s results.

(3) Please refer to Lines 257-261. We stated that “We note that poleward expansion as described here is an auroral event occurring in the initial pulse of Pi2 pulsations. In the succeeding pulses in the Pi2 wave trains, auroras are composed of poleward surge propagating at the poleward boundary of auroral zone (PBAS) [Saka et al., 2012]. We suppose that PBASs may be directly correlated to the reconnection processes inherent in the plasma sheet. This topic will be explored in another paper.”

Comment 10:

“1) Introduction

a) Describe phenomenologically what a substorm is both from an auroral point of view and from a tail point of view. This should not just cite the author's work from a few years ago or papers from 40-60 years ago. It should also be extensive enough to demonstrate to the reader that the author has a good grasp of what the current understanding is. The present manuscript does not convey this at all. This should be more than a quote about the importance of aurora from Oguti or a reference to Akasou's 1960's papers.

b) Describe what models are currently accepted to describe these observations. (Yes they exist and there is more than one.) Again don't just cite the author's work from a few years ago or papers from 40-60 years ago.

b) Have a section on a statement of the specific unresolved issue to be targeted here. What is the current state of understanding on the poleward/equatorward issue in particular? What are the successes/deficiencies in these ideas? Why does it make sense to dismiss them? Or to modify them?

c) briefly describe what the current paper will do to resolve this problem, with a short outline of the sections to follow and how they flow.”

Response:

Please refer to section 1 for the introduction. It was rewritten to include above comment. The BBF triggering has been accepted substorm model in the literature. I emphasized in the manuscript that auroral ionosphere becomes more active in this context.

Comment 11:

“2) Proposed new model type of section. Describe the scenario and how it can lead to poleward propagation.

a) Sections on the scenario -- these are largely written already, but need to be drastically cleaned up to read more coherently. (With fewer definitive assertions and more suggestions.)”

Response:

Please refer to sections 2, 3, 4, and 5 for proposed scenario. We suggest that plasma compression in the ionosphere implemented the ionosphere active. The active ionosphere includes a nonlinear evolution of the compressed ionosphere, field-aligned currents to satisfy the quasi-neutrality of the

ionosphere, and parallel potentials associated with the excitation of an ion acoustic wave. We studied how the active ionosphere created auroral expansion.

Comment 12:

“3) Discussion-like sections

a) Describe what types of poleward propagation it can address? Note that it is totally unbelievable that this scenario can address all facets of poleward motion. Why? Because at the extreme end, the poleward propagating part of the bulge eventually forms a double-oval like configuration that must engage extremely large regions of the magnetotail. Unless the density-accumulation concept proposed here can engage most of the nightside magnetosphere, it seems insufficient.

b) Can the scenario yield explosive poleward motion? Why, why not? Etc.. (Note that tailward-propagating tail-lights doesn't seem explosive.)

c) How does this scenario relate to other ideas and how does it explain all of the observations that were described in the first section? E.g. flow-braking? What has been neglected for the current scenario to ignore flow-braking? Etc..”

Response:

(a) Please refer to Lines 257-261; “we note that poleward expansion as described here is an auroral event occurring in the initial pulse of Pi2 pulsations. In the succeeding pulses in the Pi2 wave trains, auroras are composed of poleward surge propagating at the poleward boundary of auroral zone (PBAS) [Saka et al., 2012]. We suppose that PBASs may be directly correlated to the reconnection processes inherent in the plasma sheet. This topic will be explored in another paper.”

(b) Characteristic speed of the auroral formation was reported to be 5-8 km/s independent of the spatial scale of the auroras [Oguti, Metamorphoses of aurora, Memoirs of National Institute of Polar Research: series A, aeronomy, 12, 1-101, 1975]. If we can use this velocity as a speed of poleward expansion, the total electric fields of the order of 300 mV/m may be required in the auroral ionosphere. The electric fields from DF (5 mV/m at B=30 nT) create incident electric fields of the order of 200 mV/m by the projections into the auroral ionosphere (B=50000 nT). If the Alfvén conductance was larger than the height integrated Pedersen conductance, total electric fields (sum of incident and reflected electric fields) may increase to 300 mV/m. These electric fields produce poleward expansion

velocity of the order of 6 km/s. This is consistent with Oguti's results.

(c) The BBF triggering has been accepted substorm model in the literature. I emphasized in the manuscript that auroral ionosphere becomes active in this context. The active ionosphere was applied to describe the auroral expansion.

Comment 13:

"3) Conclusion/discussion on where the scenario is most likely to fit into the overall picture. My feeling is that it might provide some explanation of the poleward motion during situations where streamers reach the equatorward part of the oval and possibly during some early initial phase of the contact breakup type events. (Note that the first disturbance is not a substorm at all and the second may only relate to the early phases of a complete substorm.) I rather suspect that the scenario is extremely unlikely to be able to explain the entire typical substorm sequence. A competent description of "what a substorm is" in the first section will, almost certainly, lead to the later part of this conclusion. Without that first section, conclusions like the one in the present manuscript are simply not supported."

Response:

We described the auroral expansion in terms of acoustic regime because the ionosphere becomes active by the compression. If the field line thinning developed enough in the growth phase, intense electric fields in DF reached lowest latitudes to initiate active ionosphere. If the thinning was not enough, weak electric fields initiate weak or no activities at intermediate latitudes.

2

3

4 Osuke Saka

5

6 Office Geophysik, Ogoori, Japan

7

8

9 **Abstract**

10 Transient westward electric fields from the magnetosphere generate equatorward plasma drifts of the
11 order of kilometers per second in the auroral ionosphere. This flow channel extends in north-south
12 directions and is produced in the initial pulse of Pi2 pulsations associated with the field line
13 dipolarization. Drifts in the ionosphere of the order of kilometers per second that accumulated plasmas
14 at the low latitude end of the flow channel are of such large degree that possible vertical transport
15 effects (including precipitation) along the field lines may be ignored. **We suggest that plasma
16 compression in the ionosphere implemented the ionosphere active. The active ionosphere
17 includes a nonlinear evolution of the compressed ionospheric plasmas, field-aligned currents to
18 satisfy the quasi-neutrality of the ionosphere, and parallel potentials associated with the
19 excitation of an ion acoustic wave. We will study how the active ionosphere created auroral
20 expansion.**

21

22 **1. Introduction**

23 “Auroras and solar corona observed at the solar eclipse are optical phenomena unique in space physics.
24 With enough knowledge about the underlying physical processes, once auroras have been captured by
25 a highly sensitive imager, they provide an unexpected wealth of information about plasma
26 environment of the Earth” [Oguti, 2010]. Plasma drifts in the ionosphere observed by the balloon-
27 measured electric fields [Kelley et al., 1971], by the Ba releases [Haerendel, 1972] and by radar

28 observations [Nielsen and Greenwald, 1978] did not match the expanding trajectories of auroras.
29 These were observed in all-sky images as violent motion of auroras propagating poleward [Akasofu
30 et al., 1966] and contact breakups initiated at the nearest approach to the hydrogen arc [Oguti, 1973].
31 **To account for the difference in propagation directions, it was suggested that the primary sources**
32 **of auroral particles are in the magnetospheric plasmas and they developed poleward in terms of**
33 **propagation of rarefaction wave in the tail [Chao et al., 1971; Liu et al., 2012], tailward**
34 **regression/braking of the fast earthward flows referred to as BBFs [Shiokawa et al., 1997;**
35 **Haerendel, 2015], and onset instability of inner plasma sheet pressure [Nishimura et al., 2010].**
36 **It is suggested that substorm expansion was initiated and amplified at the substorm onset by the**
37 **BBFs arriving at the inner boundary of plasma sheet from the tail [Kepko et al., 2004;**
38 **Angelopoulos et al., 2008; Machida et al., 2009].**

39 **We will show that the electric fields in the dipolarization front (DF) [Runov et al., 2011]**
40 **amplified by the projections into the auroral ionosphere yield the compressibility in auroral**
41 **ionosphere. The compressibility initiates the active ionosphere and leads to an alternative**
42 **scenario of the poleward expansion of auroras. In this paper, field line reconfiguration at**
43 **dipolarization onset and associated auroral breakups will be summarized in section 2. In section**
44 **3, we will show that the auroral ionosphere becomes compressive transiently during**
45 **dipolarization. Section 4 will discuss generation of an ion acoustic wave for creating parallel**
46 **potentials in the topside ionosphere. Poleward expansion of discrete auroras will be discussed in**
47 **section 5 in terms of a nonlinear evolution of the accumulated plasmas in the ionosphere. In the**
48 **final section (section 6), we summarize our results and apply “the active ionosphere” to the**
49 **nonconjugate auroras.**

50

51 **2. Auroras and field line reconfiguration associated with Pi2**

52 In the waveform of Pi2 pulsations, poleward expansion of auroras arising out of the onset arc was
53 observed in the initial pulse of Pi2 pulsations [Saka et al., 2012]. **Statistical study of field line**
54 **inclinations at geosynchronous orbit for the intervals from 120-min prior to the Pi2 onset (T-**

55 **120) to 60-min after the onset (T+60) is presented in Figure 1 (reproduced from [Saka et al.,**
56 **2010]).** The inclination is measured positive northward from the D-V plane of the HVD coordinates.
57 H is positive northward parallel to dipole axis, V is radial outward, and D is dipole east. It shows that
58 field line inclination at geosynchronous orbit (Goes5/6 at $285^\circ/252^\circ$ in geographic coordinates)
59 decreased continuously in the growth phase and attained minimum inclination angles, $33.6^\circ/49.4^\circ$,
60 2-min prior to the initial peak of Pi2 amplitudes. These inclination angles are smaller than $57.5^\circ/63.8$
61 $^\circ$ estimated by the IGRF (International Geomagnetic Reference Field) model but rather fit the T89
62 model [Tsyganenko, 1989] of $K_p=4$ ($34.2^\circ/45.0^\circ$). These field lines at the geosynchronous altitudes
63 can be mapped to auroral ionosphere at $63.4^\circ\text{N}/62.7^\circ\text{N}$ in geomagnetic coordinates by T89 for $K_p=4$.
64 **From these estimations, we postulate that BBFs reaching geosynchronous orbit activated**
65 **preonset auroras at $63.4^\circ\text{N}/62.7^\circ\text{N}$ by the transmission of electric fields from the dipolarization**
66 **front (DF) embedded in the initial pulse of the BBFs [Runov et al., 2011]. These transient electric**
67 **fields were observed by the geosynchronous satellites as the convection enhancement of the**
68 **plasma sheet electrons due to local breakdown of the last open trajectories of plasma sheet**
69 **electrons [Thomsen et al., 2002]. The convection enhancement occurred in all-sky image**
70 **coincident with the onset of bead-like rippling that leads to the breakups at the equatorward**
71 **latitudes [Saka et al., 2014]. In the following Pi2 pulses, an auroral surge was observed in all-sky**
72 **images between 66°N to 74°N in geomagnetic latitudes referred to as Poleward Boundary Aurora**
73 **Surge (PBAS) [Saka et al., 2012]. They propagated eastward or westward at the poleward boundary**
74 **of the auroral zone and were interpreted as an auroral manifestation of flow bifurcation of BBFs. In**
75 **this onset scenario, the field line dipolarization finished in the initial pulse of the Pi2 pulsations,**
76 **increasing field line inclination in a step-like manner for Goes5, and generating transient pulses for**
77 **Goes6. The convection surge occurred once in the initial pulse of BBFs (DF) but is not repeated**
78 **in the following pulses in the BBF train. This correlation suggests that auroral breakup may not**
79 **repeat in the Pi2 wave packet but occurred at its initial pulse.**

80

81 3. Horizontal plasma flows in the ionosphere

82 We assume that westward electric fields in the DFs that reached the vicinity of geosynchronous
83 altitudes were transmitted along the field lines to the auroral ionosphere by the guided poloidal mode
84 [Radoski, 1967]. The electric fields in DFs would be amplified during the projection into the
85 ionosphere over 100 mV/m and created an equatorward flow through $E \times B$ drift of the order of
86 kilometers per second in the auroral ionosphere. Electric fields of the order of 100 mV/m generate
87 these high velocity flows in the ionosphere. The flows would be confined in a channel expanding
88 north-south in the midnight sector. The low-latitude end of the flow channel was at the latitudes of the
89 onset arc. The high-latitude end may not expand beyond the poleward boundary of auroral zone.
90 **Longitudinal width of the flow channel may form a streamer [e.g., Nishimura et al, 2010] and**
91 **develops after the breakups in about 1 to 2 hours of local time (~1000 km along 65° N)**
92 **corresponding to horizontal scale size of plasma flow vortices associated with Pi2 [Saka et al.,**
93 **2014].**

94 In the flow channel, drift across the magnetic fields for the j -th species ($\mathbf{U}_{j\perp}$) can be written in
95 the F region as [Kelley, 1989],

$$96 \quad \mathbf{U}_{j\perp} = \frac{1}{B} \left[\mathbf{E} - \frac{k_B T_j}{q_j} \frac{\nabla n}{n} \right] \times \hat{\mathbf{B}}. \quad (1)$$

97 Here, \mathbf{E} denote westward electric fields in the flow channel and $\hat{\mathbf{B}}$ denotes a unit vector of the
98 magnetic fields B , downward in the auroral ionosphere. Symbols k_B , T_j , q_j , and n are the Boltzmann
99 constant, temperature of the j -th species, charge of the j -th species, and density of electrons (ions),
100 respectively. The electric field of the order of 100 mV/m exceeded the diffusion (second term) by three
101 orders of magnitudes in low temperature ionosphere. The $E \times B$ drift predominated in the F region
102 and diffusion term may be ignored. In the E region, drift trajectories may be written [Kelley, 1989] for
103 electrons by,

$$104 \quad \mathbf{U}_{e\perp} = \frac{1}{B} [\mathbf{E} \times \hat{\mathbf{B}}] \quad (2)$$

105 and for ions by,

106
$$\mathbf{U}_{i\perp} = b_i[\mathbf{E} + \kappa_i \mathbf{E} \times \hat{\mathbf{B}}]. \quad (3)$$

107 Here, b_i is mobility of ions defined as $\Omega_i/(B\nu_{in})$, κ_i is defined as Ω_i/ν_{in} . Symbols Ω_i and
 108 ν_{in} are ion gyrofrequency and ion-neutral collision frequency, respectively. $\hat{\mathbf{B}}$ denotes a unit vector
 109 of the magnetic fields B . To derive equations (2) and (3), pressure gradient term (diffusion) was
 110 again ignored. In the E region ($\kappa_i = 0.1$), although the first term of (3) exceeds the second term by
 111 one order of magnitudes, plasma accumulation in equatorward latitudes by the imposed westward
 112 electric fields was produced by equation (2) for electrons and the second term in (3) for ions. However,
 113 electron accumulation in lower latitudes increased southward electric fields and simultaneously ion
 114 drifts in the first term of (3). If the southward electric fields grew to exceed the westward electric fields
 115 by an order of magnitudes, ion drifts in the first term of (3) and electron drifts in (2) balanced to satisfy
 116 the quasi-neutrality. This is equivalent to the generation of the Pedersen currents in the ionosphere.
 117 Thus, electrostatic potential is generated in the E region, positive in poleward and negative in
 118 equatorward. The Pedersen currents would have closed to the field-aligned current (FAC), upward
 119 from the negative potential region and downward into the positive potential region to sustain the steady
 120 state electrostatic potential produced in the ionosphere. Plasma drifts in the ionosphere, both in E and
 121 F regions, create a cavity in the high-latitude end of the flow channel and accumulate density at the
 122 low-latitude end of the flow channel. We will focus on the density accumulation in the flow channel
 123 and discuss vertical transport of these accumulated materials. The development of the cavity in the
 124 flow channel may be the subject of another paper.

125

126 **4. Vertical plasma flows in the ionosphere**

127 A transient compression of the ionospheric plasmas at the low-latitude edge of flow channel
 128 would excite the ion acoustic wave in the ionosphere travelling along the field lines upward and
 129 downward directions from the density peak of the F region. Figure 2 shows altitude distribution of the
 130 pre-onset density profile of electrons (black) and density profile caused by the accumulation in red.
 131 The accumulation doubled the electron density profile from 90 km to 1000 km in altitudes. Electron

132 density profile in black was plotted using sunspot maximum condition in nightside given in Prince and
 133 Bostic (1964). The travelling ion acoustic waves, upward and downward, are denoted by vertical
 134 arrows. Ion acoustic wave propagating downward may be eventually absorbed in the neutrals, while
 135 the upward wave may propagate along the field lines further upward. We will focus only on the upward
 136 travelling ion acoustic wave. The ion acoustic wave produced the parallel electric fields in accordance
 137 with the Boltzmann relation [Chen, 1974],

$$138 \quad E_{\parallel} = -\frac{k_B T_e}{q} \frac{\nabla_{\parallel} n_e}{n_e}. \quad (4)$$

139 Here, k_B is Boltzmann constant, q is electron charge, T_e is electron temperature, and n_e is
 140 electron density ($n_e = n_i$). Equation (4) gives electric field strengths of the order of $0.4 \mu V / m$ and
 141 $2.0 \mu V / m$ for $T_e = 1000K$ and $T_e = 5000K$, respectively, when the e-folding distance of
 142 density dropout along the field lines was 200 km. For ions, steady-state motions exist in the ionosphere
 143 in the altitudes where ion-neutral collision frequencies exceed ion acoustic wave frequencies. In that
 144 case, parallel motions can be written as [Kelley, 1989],

$$145 \quad V_{i\parallel} = b_i E_{\parallel} - D_i \frac{\nabla_{\parallel} n}{n} - \frac{g}{v_{in}}. \quad (5)$$

146 Here, b_i and D_i denote mobility and diffusion coefficient of ions defined by $\frac{q_i}{M_i v_{in}}$ and

147 $\frac{k_B T_i}{M_i v_{in}}$, respectively. Symbols, M_i , q_i , v_{in} , and g are ion mass, electric charge of ions, ion-

148 neutral collision frequency, and gravity, respectively. Ion-neutral collision frequencies from 400 km
 149 to 1000 km in altitudes were plotted in Figure 3 using nighttime sunspot maximum condition in
 150 Prince and Bostick (1964). Frequencies of ion acoustic wave were calculated by substituting
 151 wavelength of ion acoustic wave into the dispersion relation. The wavelength was assumed to be
 152 identical to initial accumulation distance along the field lines. We chose two cases of 1000 km and
 153 4000 km. Phase velocity of the ion acoustic wave of the order of 1600 m/s for the electron
 154 temperatures of 5000K yields the wave frequencies of $1.6 \times 10^{-3} s^{-1}$ for the wavelength of 1000 km

155 and $4.0 \times 10^{-4} s^{-1}$ for 4000 km. These frequencies were overlaid in Figure 3. Steady-state ion
156 motions can be adopted up to 800 km, for a wavelength over 1000 km.

157 Altitude profile of steady-state ion flows were evaluated substituting 1000K for ion temperatures
158 and the same e-folding distance in equation (4). Ions are oxygen and parallel electric fields are given
159 by the equation (4). A snapshot of the velocity profile in altitudes from 400 km to 800 km is shown
160 in Figure 4 for the two cases of electron temperatures, 5000K for black dots and 1000K for red dots.
161 For the low temperature case (1000k), there occurred no ion upflow because the parallel electric
162 fields could not overcome gravity. We suggest that electron temperatures over 2700K would be
163 needed to excite ion upflow. When electron temperature was set to 5000K, ion velocity 15 m/s at 400
164 km in altitudes increased rapidly to 1369 m/s at 800 km. The altitude profile of the flow velocity in
165 Figure 4 matched Type 2 ion outflow observed by EISCAT radar [Wahlund et al., 1992]. We conclude
166 that the ion upflow in topside ionosphere was caused primarily by the parallel electric fields excited
167 by the upward travelling ion acoustic wave. Below 600 km in altitudes, upflow velocity was one-to-
168 two orders of magnitudes smaller than the equatorward drift in the flow channel. Upflow velocity
169 became comparable to the horizontal drift over 800 km in altitudes and exceeded the phase velocity
170 of ion acoustic wave. Parallel velocity that prevailed the ion acoustic phase velocity may excite a
171 shock at the topside ionosphere. A part of them developed to ion acoustic double layers [Sato and
172 Okuda, 1980; Hasegawa and Sato, 1982; Hudson et al., 1983; Ergun et al., 2002] and were observed
173 at the altitudes of 6000 – 8000 km [Mozer et al., 1976; Temerin et al., 1982]. Those ion acoustic
174 double layers would have produced parallel potential structures referred to as inverted-V type electric
175 fields.

176

177 **5. Nonlinear evolution of the horizontal flows**

178 Accumulation of electrons and ions occurred at the equatorward end of the flow channel. We can
179 estimate a rate of accumulation by the following relation,

$$180 \quad \frac{\Delta n}{\Delta t} = -n_0 \frac{\Delta U}{\Delta x} . \quad (6)$$

181 Here n is plasma density, U denotes drift velocity in the flow channel in x . Substituting
182 $\Delta U = 10^3 \text{ m s}^{-1}$ and $\Delta x = 10^4 \text{ m}$, we have $\frac{\Delta n}{\Delta t} = 10^{10} \text{ m}^{-3} \text{ s}^{-1}$ for the background density
183 $n_0 = 10^{11} \text{ m}^{-3}$. This gives density pileup of the order of $\frac{\Delta n}{n_0} = 100\%$ in ten seconds. If the
184 equatorward drift in the flow channel is an order of 10^3 m/s ($E=100 \text{ mV/m}$ in auroral ionosphere) and
185 electron production by the precipitation do not exceed the accumulation rate which was 100% of the
186 background density in ten seconds, both outflows and precipitation may not bring significant changes
187 to the flux carried by $E \times B$ drift in the flow channel. We then approximate one dimensional (along
188 the drift path in x) conservation equation in the flow channel.

$$189 \quad \frac{\partial n}{\partial t} + \frac{\partial}{\partial x}(nU) = 0 \quad (7)$$

190 A question arises regarding maximum accumulation of plasmas at the equatorward end of the flow
191 channel because accumulation is limited. One possible mechanism to suppress accumulation may be
192 associated with the ionospheric screening that decreased the amplitudes of penetrated (total) westward
193 electric fields by the increasing ionospheric conductivities. In a two-dimensional ionosphere with
194 uniform height-integrated conductivity, total electric fields E given by a sum of the incident (E_i) and
195 reflected westward electric fields may be written as $E = \left(2\Sigma_A / (\Sigma_A + \Sigma_p)\right) E_i$, where Σ_A and
196 Σ_p are Alfvén conductance defined by $1/\mu_0 V_A$ and height-integrated Pedersen conductance in the
197 ionosphere, respectively [Kan et al., 1982]. Symbols μ_0 and V_A denote magnetic permeability in
198 vacuum and Alfvén velocity, respectively. Amplitude ratio of total electric fields to incident electric
199 fields is a function of conductance ratio of Pedersen and Alfvén; $E/E_i = 2$ for a low conductivity of
200 the ionosphere satisfying $\Sigma_p/\Sigma_A \ll 1$, and $E/E_i = 0$ for a high conductivity of the ionosphere
201 satisfying $\Sigma_p/\Sigma_A \gg 1$. Noting that Σ_p is proportional to the plasma density in the ionosphere, the
202 total electric fields monotonically decreased with increasing plasma densities caused by accumulation
203 itself and by the precipitations associated with the auroral activity. Another explanation may be

204 suggested in the polarization electric fields (eastward) produced by the accumulation itself. These
 205 electric fields grew quickly with density accumulation and decreased the incident electric fields
 206 (westward) by the superposition. In addition to the above scenarios, we surmise that excess
 207 accumulation of the ionospheric plasmas may be suppressed through the term, $(\mathbf{U} \cdot \nabla)\mathbf{U}$, in the
 208 equation of motion. From the ionospheric screening process discussed above, we tentatively assume
 209 that flow velocity U is a function of the density n . Then the conservation equation (7) may be written
 210 as,

$$211 \quad \frac{\partial n}{\partial t} + \frac{\partial}{\partial x} Q(n) = 0. \quad (8)$$

212 Here, $Q(n)$ is a mass flux defined by $Q(n)=nU(n)$. This relation can be reduced to nonlinear wave
 213 equation,

$$214 \quad \frac{\partial n}{\partial t} + c(n) \frac{\partial n}{\partial x} = 0. \quad (9)$$

215 Here $c(n)$ is a wave propagation velocity defined by $c(n) = U(n) + nU'(n)$, $U(n)$ is a drift velocity
 216 in the flow channel, and $U'(n)$ denotes braking/acceleration of the drift velocity by increasing and
 217 decreasing density. The equation (9) is often referred to as propagation of “kinematic waves” to
 218 describe traffic flow [Lighthill and Whitham, 1955]. In the following, we use dimensionless units
 219 normalized by U_m , and n_m . Here, U_m and n_m denote maximum drift velocity at $n=0$ and maximum
 220 density for complete stops of the drift, respectively. Assuming a constant braking in the flow channel,
 221 we define U by a linear function of density n as $U(n)=1-n$. Noting that $Q'(n)=c(n)$, this relation is
 222 reduced to the equation, $Q(n)=n(1-n)$, identical to the case for the traffic flow [Whitham, 1999]. Both
 223 the U and Q are plotted in Figure 5A as a function of n . A nonlinear evolution of the density waves is
 224 presented in Figure 5B by the characteristic curves. In the case of vehicles in traffic, the initial flows
 225 started from $n=0$ and stopped at $n=1.0$ by the tailback of cars. For the case of the ionosphere, the
 226 ionospheric density started from a finite density, $n=0.3$ in Figure 5B, and increased to $n=1.0$ to
 227 terminate the flow by the full screening. The nonlinear evolution of the density profile in time is shown
 228 in Figure 5B in colors from black ($T=T_1$), red ($T=T_2$), green ($T=T_3$), blue ($T=T_4$), and to purple ($T=T_5$).

229 After $T=T_5$, the waves propagate upstream (poleward) as a shock. The shock velocity, V , is given as
230 [Whitham, 1999],

$$231 \quad V = \frac{Q(n_2) - Q(n_1)}{n_2 - n_1}. \quad (10)$$

232 Here, subscript 1 is for the values ahead shock and subscript 2 is for the values behind. Noting that
233 $Q(n_2)=0$ and substituting $Q(n_1)=n_1(n_2-n_1)$, the equation (10) can be reduced to $V = -n_1$ in
234 dimensionless unit. The propagation velocity of the shock is related to the densities ahead. For the
235 case of $n=0.3$ in Figure 5B, shock velocity can be estimated to be $-0.3U_m$. Here, U_m denotes maximum
236 drift velocity in the ionosphere where ionospheric screening effects vanished by the condition,
237 $\Sigma_p/\Sigma_A \ll 1$. The shock velocity may be of the order of kilometer per second, comparable but
238 opposite to the equatorward drift in the flow channel.

239

240 6. Summary and Discussion

241 **We proposed that the localized electric field drift introduced compressibility in the auroral**
242 **ionosphere, which in turn generated field-aligned currents in the ionosphere for the quasi-**
243 **neutrality, ion acoustic wave for parallel acceleration, and auroral expansions by nonlinear**
244 **evolution of the ionospheric compression. We called the compressive ionosphere an active**
245 **ionosphere.**

246 **We apply this active ionosphere to describe the asymmetry of discrete auroras in sunlit and**
247 **dark hemispheres in the nightside sector (nonconjugate auroras). We suggest that asymmetry of**
248 **the Pedersen conductance in sunlit and in dark ionosphere leads to the nonconjugate auroras.**
249 **Weak electric fields in the sunlit auroral ionosphere would have caused a weak compressibility**
250 **from which ion acoustic wave may not be excited or excited with only weak parallel potentials.**
251 **This condition may reduce the occurrence probability of the discrete auroras and average energy**
252 **of precipitating electrons in the sunlit hemisphere as exemplified in [Newell et al., 1996; Liou et**
253 **al., 2001]. Weaker electric fields in the sunlit ionosphere may also require a longer interval to**
254 **accumulate enough plasmas to excite ion acoustic wave. Such an instance is described in [Sato**

255 et al., 1998] where auroral breakups in sunlit ionosphere are delayed those in the dark
256 hemisphere.

257 Finally, we note that poleward expansion as described here is an auroral event occurring in
258 the initial pulse of Pi2 pulsations. In the succeeding pulses in the Pi2 wave trains, auroras are
259 composed of poleward surge propagating at the poleward boundary of auroral zone (PBAS)
260 [Saka et al., 2012]. We suppose that PBASs may be directly correlated to the reconnection
261 processes inherent in the plasma sheet. This topic will be explored in another paper.

262

263 Acknowledgements

264 The author would like to express his sincere thanks to all the members of Global Aurora
265 Dynamics Campaign (GADC) [Oguti et al., 1988]. We also gratefully acknowledge STEP Polar
266 Network (<http://step-p.dyndns.org/~khay/>). Geomagnetic coordinates and footprints of the satellites
267 are available at the Data Center for Aurora in NIPR (<http://polaris.nipr.ac.jp/~aurora>)

268

269

270

271 References

272 Akasofu, S.-I., Kimball, D.S., and Meng, C.-I.: Dynamics of the aurora-VII, Equatorward motions and
273 the multiplicity of auroral arcs, J.Atmos.Terr.Phys., 28, 627-635, 1966.

274 Angelopoulos, V., et al.: Tail reconnection triggering substorm onset, Science, 321, 931, 2008.

275 Chao, J.K., Kan, J.R., Lui, A.T.Y., and Akasofu, S.-I.: A model for thinning of the plasma sheet,
276 Planet.Space Sci., 25, 703-710, 1977.

277 Chen, F.F.: Introduction to plasma physics, Plenum Press, New York, 1974.

278 Ergun, R.E., et al.: Parallel electric fields in the upward current region of the aurora: Numerical
279 solutions, Physics of Plasmas, 9, 3695-3704, 2002.

280 Haerendel, G.: Plasma drifts in the auroral ionosphere derived from Barium release, in Earth
281 magnetospheric processes, B.M. McComac (ed), D.Reidel Publishing Company, 246-257,
282 1972.

283 Haerendel, G.: Substorm onset: Current sheet avalanche and stop layer, *J.Geophys.Res.*, 120,
284 doi10.1002/2014JA020571, 2015.

285 Hasegawa, A., and Sato, T.: Existence of a negative potential solitary-wave structure and formation of
286 a double layer, *Phys.Fluids*, 25, 632-635, 1982.

287 Hudson, M.K., Lotko, W., Roth, I., and Witt, E.: Solitary waves and double layers on auroral field
288 lines, *J.Geophys.res.*, 88, 916-926, 1983.

289 Kan, J.R., Longenecker, D.U., and Olson, J.V.: A transient response of Pi2 pulsations, *J.Geophys.Res.*,
290 87, 7483-7488, 1982.

291 Kelley, M.C., Starr, J.A., and Mozer, F.S.: Relationship between magnetospheric electric fields and
292 the motion of auroral forms, *J.Geophys.Res.*, 76, 5256-5277, 1971.

293 Kelley, M.C.: The earth's ionosphere: plasma physics and electrodynamics, Academic Press, Inc.,
294 1989.

295 Kepko, L., Kivelson, M.G., McPherron, R.L., and Spence, H.E.: Relative timing of substorm onset
296 phenomena, *J.Geophys.Res.*, 109, doi:10.1029/2003JA010285, 2004.

297 Lighthill, M.J., and Whitham, G.B.: On kinematic waves. II. A theory of traffic flow on long crowded
298 roads, *Proc. R. Soc. Lond. A*, 229, 317-345, 1955.

299 Liou, K., Newell, P.T., and Meng, C.-I.: Seasonal effects on auroral particle acceleration and
300 precipitation, *J.Geophys.Res.*, 106,5531-5542, 2001.

301 Liu, W.W., Liang, J., Donovan, E.F., and Spanswick, E.: If substorm onset triggers tail reconnection,
302 what triggers substorm onset, *J.Geophys.Res.*, 117, doi:10.1029/2012JA018161, 2012.

303 Machida, S., et al.: Statistical visualization of the arth's magnetotail based on Geotail data and the
304 implied substorm model, *AnnGeophys.*, 27, 1035-1046, 2009.

305 Mozer, F.S., Carlson, C.W., Hudson, M.K., Torbert, R.B., Parady, B., Yatteau, J., and Kelley, M.C.:
306 Observations of paired electrostatic shocks in the polar magnetosphere, *Phys.Rev.Lett.*, 38,
307 292-295, 1977.

308 Newell, P.T., Meng, C.I., and Lyons, K.M.: Suppression of discrete aurorae by sunlight, *Nature*, 381,
309 766-767, 1996.

310 Nielsen, E., and Greenwald, R.A.: Variations in ionospheric currents and electric fields in association
311 with absorption spikes during substorm expansion phase, *J.Geophys.Res.*, 83, 5645-5654,
312 1978.

313 Nishimura, Y., et al., Preonset time sequence of auroral substorms: Coordinated observations by all-
314 sky imagers, satellites, and radars, *J.Geophys.res.*, 115, doi:10.1029/2010JA015832, 2010.

315 Oguti, T.: Hydrogen emission and electron aurora at the onset of the auroral breakup, *J.Geophys.Res.*,
316 78, 7543-7547, 1973.

317 Oguti, T., Kitamura, T., and Watanabe, T.: Global aurora dynamics campaign, 1985-1986,
318 *J.Gemag.Geolectr*, 40, 485-504, 1988.

319 Oguti, T.: Introduction to auroral physics (in Japanese), Laboratory for Solar-Terrestrial Environment,
320 Nagoya University, 2010.

321 Prince, Jr., C.E., and Bostick, Jr., F.X.: Ionospheric transmission of transversely propagated plane
322 waves at micropulsation frequencies and theoretical power spectrums, 69, 3213-334, 1964.

323 Radoski, H.R.: Highly asymmetric MHD resonances: The guided poloidal mode, *J.Geophys.Res.*, 72,
324 4026-4027, 1967.

325 Runov, A., Angelopoulos, V., Zhou, X.-Z., Zhang, X.-J., Li, S., Plaschke, F., and Bonnell, J.: A
326 THEMIS multicase study of dipolarization fronts in the magnetotail plasma sheet,
327 *J.Geophys.Res.*, 116, A05216, doi:10.1029/2010JA016316, 2011.

328 Saka, O. Hayashi, K., and Thomsen, M.: First 10 min intervals of Pi2 onset at geosynchronous altitudes
329 during the expansion of energetic ion regions in the nighttime sector, *J.Atmos.Solar Terr.Phys.*,
330 72, 1100-1109, 2010.

331 Saka, O., Hayashi, K., and Koga, D.: Periodic aurora surge propagating eastward/westward at
332 poleward boundary of aurora zone during the first 10 min intervals of Pi2 onset, *J.Atmos.Sol.*
333 *Terr.Phys.*, 80, 285-295, doi:10.1016/j.jastp.2012.02.010, 2012.

334 Saka, O., Hayashi, K., and Thomsen, M.: Pre-onset auroral signatures and subsequent development of
335 substorm auroras: a development of ionospheric loop currents at the onset latitudes, *Ann.*
336 *Geophys.*, 32, 1011-1023, 2014.

337 Sato, T., and Okuda, H.: Ion-acoustic double layers, *Phys.Rev.Lett.*, 44, 740-743, 1980.

338 Sato, N., Nagaoka, T., Hashimoto, K., and Saemundsson, T.: Conjugacy of isolated auroral arcs and
339 nonconjugate auroral breakups, *J.Geophys.res.*, 103, 11641-11652, 1998.

340 Shiokawa, K., Baumjohann, W., and Haerendel, G.: Braking of high-speed flows in the near-Earth tail,
341 *Geophys.Res.Lett.*, 24, 1179-1182, 1997.

342 Temerin, M., Cerny, K., Lotko, W., and Mozer, F.S.: Observations of double layer and solitary waves
343 in the auroral plasma, *Phys.Rev.Lett.*, 48, 1176-1179, 1982.

344 Thomsen, M.F., Korth, H., and Elphic, R.C.: Upper cutoff energy of the electron plasma sheet as a
345 measure of magnetospheric convection strength, *J.Geophys.Res.*, 107,
346 doi:10.1029/2001JA000148, 2002.

347 Tsyganenko, N.A.: A magnetospheric magnetic field model with a warped tail current sheet. *Planet.*
348 *Space Sci.*, 37, 5-20, 1989.

349 Whalund, J.-E., and Opgenoorth, H.J.: EISCAT observations of strong ion outflows from the F-region
350 ionosphere during auroral activity: preliminary results, *Geophys.Res.Lett.*, 16, 727-730, 1989.

351 Whalund, J.-E., Opgenoorth, H.J., Haggstrom, I., Winser, K.J., and Jones, G.O.: EISCAT observations
352 of topside ionospheric outflows during auroral activity: revisited, *J.Geophys.Res.*, 97, 3019-
353 3017, 1992.

354 Whitham, G.B.: *Linear and nonlinear waves*, A Wiley-Interscience Publication, JOHN WILEY &
355 SONS, INC., 1999.

356

357

358 **Figure Captions**

359 Fig. 1: Inclination angles in degrees measured positive northward from the V-D plane from 120 min
360 prior to the Pi2 onset (T-120) and to 60 min after the Pi2 onset (T+60) reproduced from Saka et al.
361 (2010). Magnetometer data of Goes 5/6 were represented in HVD coordinates, H is positive northward
362 parallel to dipole axis, V is radial outward, and D is dipole east. Epoch superposition of 30 Pi2 events
363 and mean angles calculated from them are plotted in top and in lower panels, respectively. Mean
364 inclination angle at 2-min before the initial peak of Pi2 amplitudes (T=0) was 33.6° for G5 and 49.4
365 $^\circ$ for G6 in dipole coordinate. Dipolarization was step-like at 10.3° N (Goes5), while at 7.9° N
366 (Goes6) it was composed of transient pulses.

367

368 Fig. 2: Vertical profiles from 90 km to 1000 km in altitudes of electron number density in two
369 conditions, pre-onset in black and after accumulation in red. Nighttime sunspot maximum condition
370 given in Prince and Bostic (1964) was used to plot pre-onset condition. Vertical arrows directing
371 upward and downward denote travelling ion acoustic waves propagating along the field lines from the
372 density peak of F layer.

373

374 Fig. 3: Ion-neutral collision frequency (ν_{in}) in altitudes from 400 km to 1000 km calculated using
375 nighttime sunspot maximum condition in Prince and Bostick (1964). Wave frequencies of ion acoustic
376 wave are overlaid for two wavelength, 1000 km and 4000 km along field lines (see text).

377

378 Fig. 4: Steady-state parallel velocity in altitudes for ions (oxygen) produced by parallel electric fields
379 $0.4\mu V / m$ ($T_e=1000K$) in red dots and $2.0\mu V / m$ ($T_e=5000K$) in black dots. Vertical flows in
380 altitudes from 400 km to 800 km are shown. Flow velocity is positive upward and negative downward.

381

382 Fig. 5: (A) Normalized flux(Q)-density(n) curve (thin curve) and velocity(U)-density(n) line (thick
383 line) in flow channel. Vertical scale of U - n line is shown to the right, scale of Q - n curve is to the left.
384 Dotted line at $n=0.5$ indicates the critical density where $c(n)$ vanishes; waves are stationary relative to

385 the ground. Waves propagate forward/backward at a density below/above the critical density. (B)

386 Nonlinear evolution of the density accumulation. Density increased in a step like manner from T_1 to

387 T_5 .

388

389

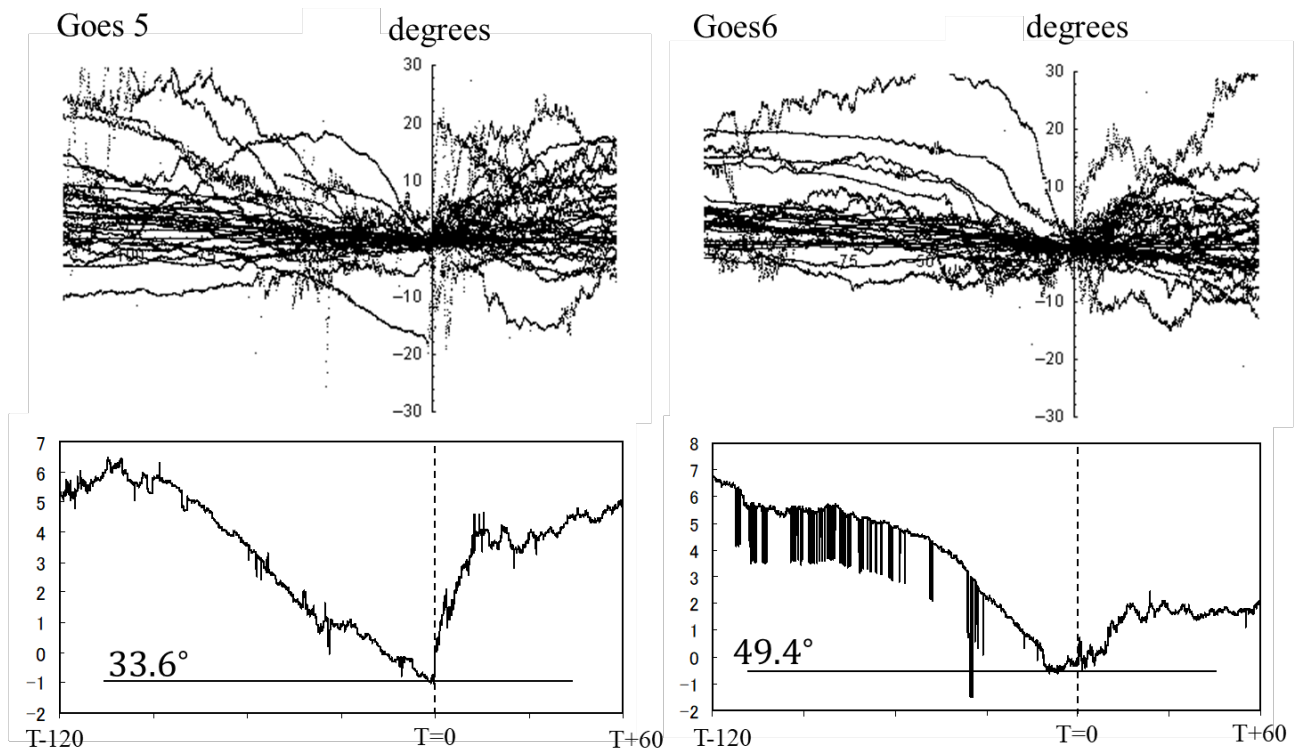


Figure 1

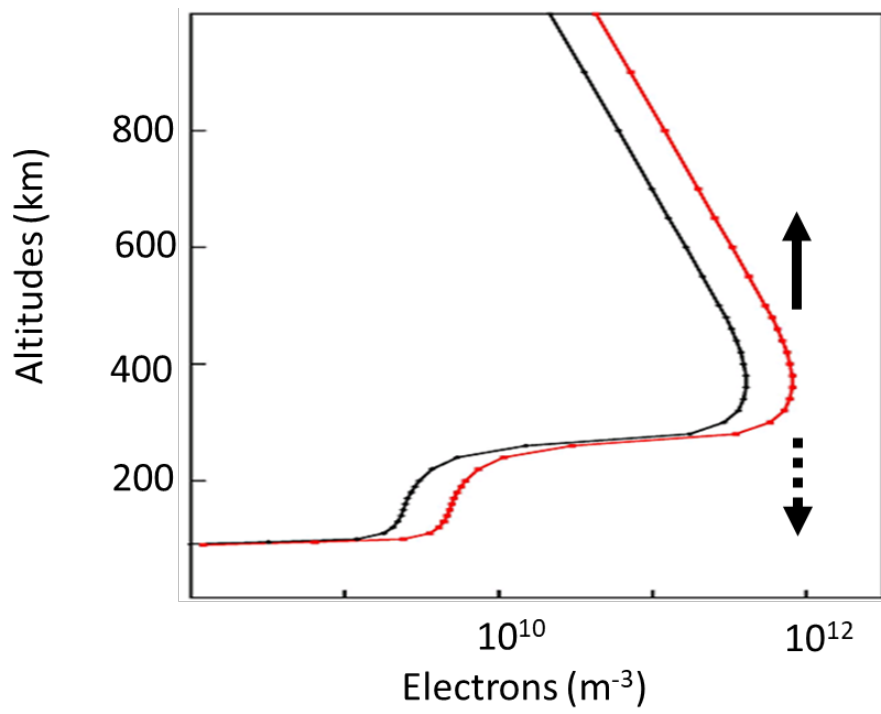


Figure 2

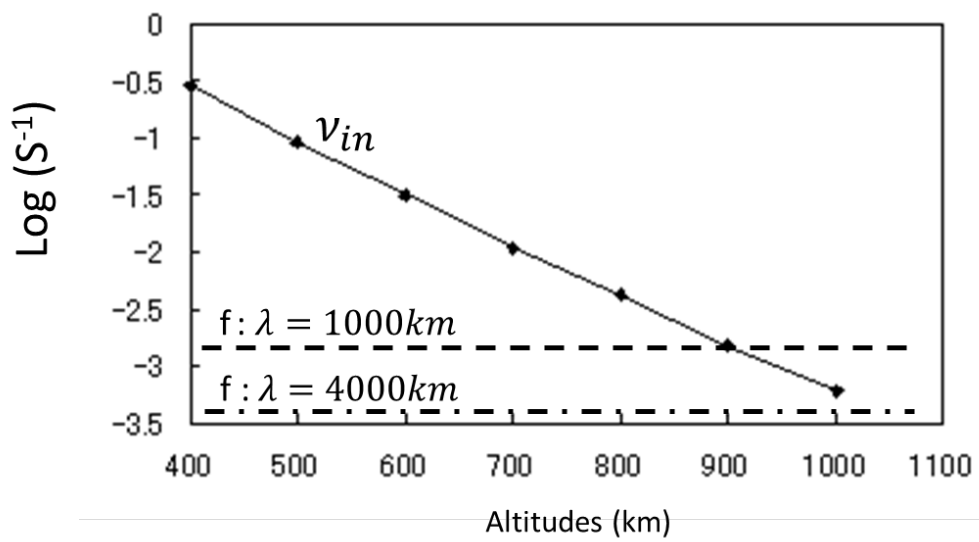


Figure 3

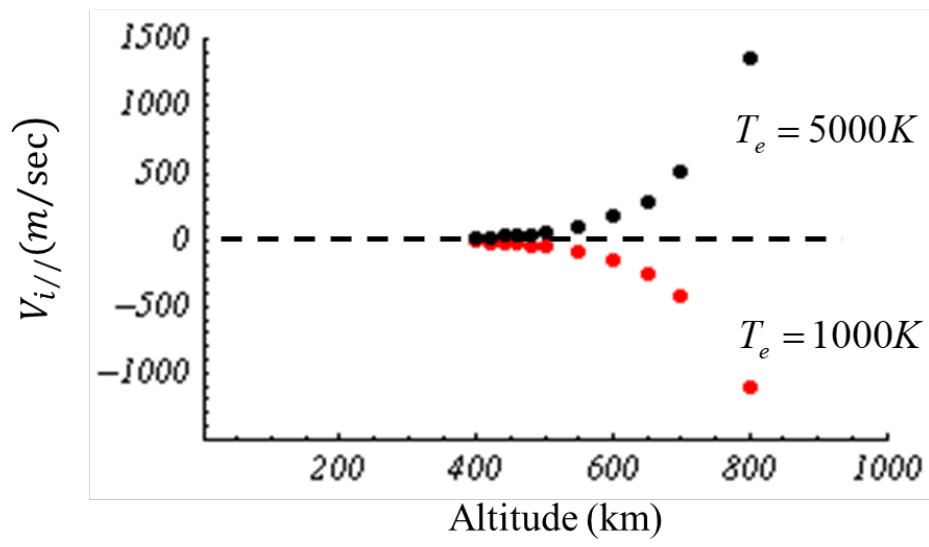


Figure 4

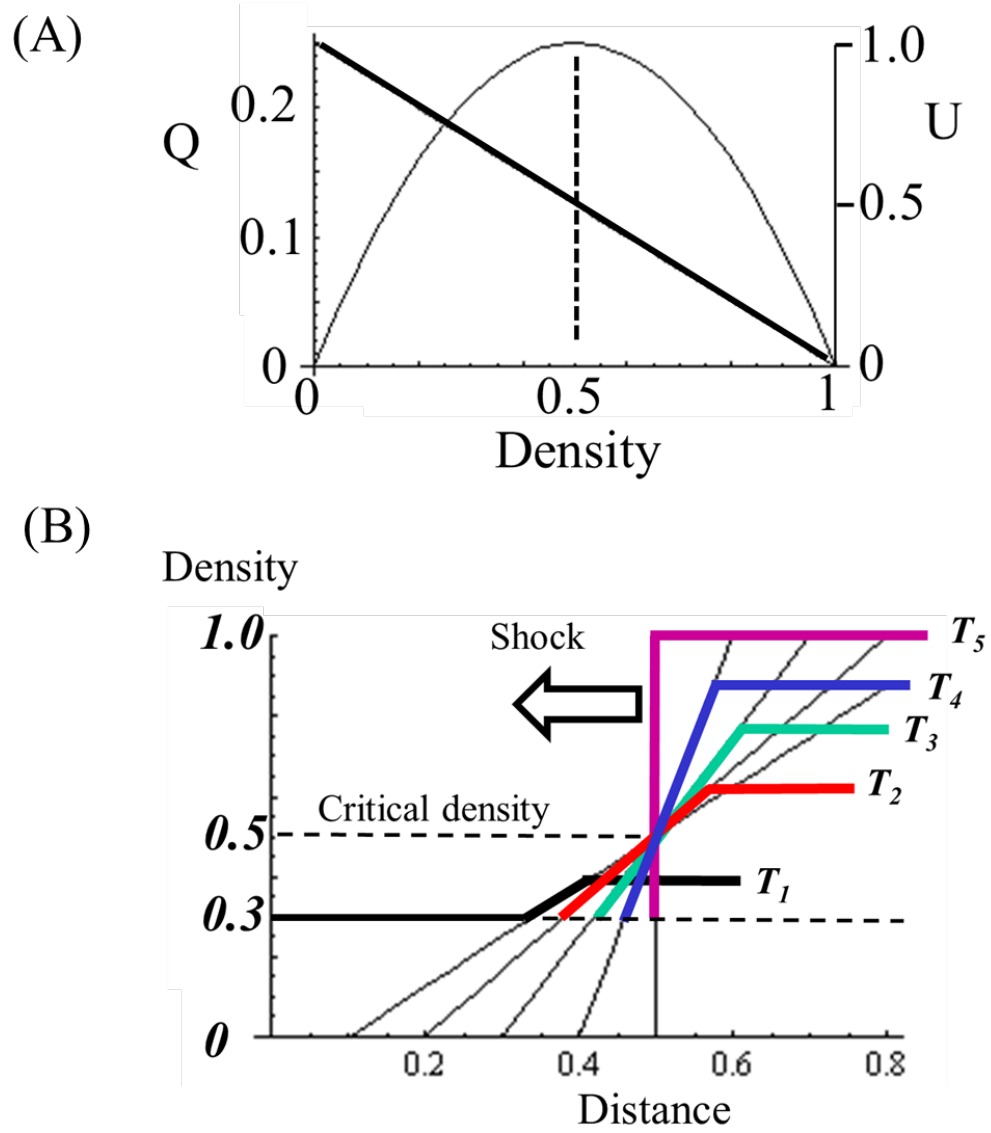


Figure 5